BIO Web of Conferences **129**, 04013 (2024) https://doi.org/10.1051/bioconf/202412904013
EMC 2024

Influence of the loss function on gradient-based iterative ptychographic reconstructions in 4D-STEM

Max Leo Leidl[1,2], Carsten Sachse[2,3], Knut Müller-Caspary[1,2]
[1]Ludwig Maximilian University of Munich, Munich, Germany, [2]Ernst Ruska-Centre, Forschungszentrum Jülich GmbH, Jülich, Germany, [3]Heinrich Heine Universitöt Düsseldorf, Düsseldorf, Germany

Background incl. aims

The noise model of a detector's counting process is known as Poisson shot noise. However, direct reconstruction algorithms like single-sideband (SSB) or Wigner-distribution deconvolution (WDD) do not assume a specific noise model. This is not the case for gradient descent-based iterative methods that allow the free choice of the loss function and, therefore, the underlying noise model. In practice the mean square error (MSE), also known as L2 loss, is often used, which assumes Gaussian white noise. This is a good approximation for the Poissonian statistics for high counts.
In contrast, the (extended) iterative engine (e)PIE assumes no specific noise model. However, Melnyk showed that ePIE can be seen as a particular case of stochastic gradient descent using the MSE Loss on the amplitudes instead of the intensities [1], which we will call the Amplitude loss function in the following. The amplitude loss can be derived from the Poisson loss function via a Taylor expansion, assuming that the specimen guess is close to the original specimen [2] and, therefore, an approximation of the Poisson loss.
The interest in using STEM for low-dose applications has grown in recent years, e.g., to examine dose-sensitive, weakly scattering specimens like covalent or metal organic frameworks (COFs/MOFs), or 2D materials. Moreover, the interest rises to explore STEM for imaging proteins and lamellae of cells [3, 4, 5], which are very dose-sensitive. Therefore, we perform a detailed analysis of the influence of the loss function on the reconstruction accuracy using a gradient descent approach for the L1, MSE, amplitude and Poisson losses.

Methods

We used a MoS_2 monolayer as a test case to perform STEM simulations and experiments. Simulations were conducted with an acceleration voltage of 60 kV and 300 kV with a convergence semi-angle of 18 mrad, in focus with a dose of 10^6 electrons per diffraction pattern. The high-dose case is of particular interest because the dark field (DF) contains very few counts.
To better understand the loss functions, we compare different virtual detector geometries. Firstly, we compare the results of the full pixelated detector for 300 kV and 60 kV. Subsequently, only an acceleration voltage of 300 kV is used. Secondly, we use the pixelated bright field (BF) disc in combination with virtual ring detectors for the dark field. Thirdly, we use only the BF disc. The results suggest that the choice of the loss function makes a

difference if a wide dynamic range of electron counts is measured. Therefore, we explore the BF disc again, but this time with more features in the BF disc introduced by an under-focused electron probe of 25 nm. Finally, we go back to the first case using 300 kV and stepwise reduce the dose to 10000 and 100 electrons per diffraction pattern for sparse-count dark field studies.

Results

Figure 1 depicts reconstruction results using different loss functions and high (left) as well as low (right panels) dose. The differences between the reconstructed objects using various loss functions are significant if the signal involves a wide dynamic range of electron counts. This applies to the high-dose case (left) in which the signal levels of the BF disc and the DF differ significantly. It is best seen in the power spectra (c) where Poisson and Amplitude losses lead to reconstructed object transmission functions containing the highest spatial frequencies, followed by the L1 loss result. Note that only the Poisson loss leads to a flat spatial frequency transfer, whereas the other methods pronounce Fourier coefficients within a band of twice the probe-formin aperture radius. The line profile in (d) exhibits the sharpest peaks for the Poisson loss. Chemical contrast between a Mo monomer and S dimer is only represented in the phase of the Poisson and amplitude loss functions, respectively.

An electron dose of 100 electrons per diffraction pattern on the right of Fig. 1 appears as a limiting case for all losses considered here, with the Poisson loss still performing best. However, the difference to the MSE loss becomes smaller than for the high-dose case.

The counts in the DF are sparse, so we used virtual ring detectors for the DF to perform an azimuthal integration to get a more robust measurement. In this case, the differences between the loss functions became smaller and the chemical contrast accessible. Excluding the dark field counts and only using the BF, all loss functions lead to comparable reconstructions because the dynamic intensity range in the BF itself is rather small. Moreover, the introduction of more features into the BF disc by an under-focus increases the dynamic range slightly, but the variation is too small to pronounce one of the loss concepts against others.

Conclusion

Our results show that the differences between the loss functions become large for a broad dynamic range of electron counts, which is the case for high-dose measurements when the BF and DF are of interest at the same time, is relevant for chemical contrast found accurately represented in the phase of the Poisson loss based reconstruction. The MSE loss assumes a constant Gaussian noise distribution and the same standard deviation for all pixels. In contrast, the standard deviation of the Poisson loss scales with the square root of the number of counts. This makes a difference for a wide dynamic range in measurements and is consistent with our results. Our results suggest that the differences between the MSE and Poisson loss become small for dose-sensitive materials because sparse counts are measured and, as a result, a very low dynamic range. However, the Poisson loss is still beneficial at high frequencies and shows a lower variance of the reconstruction. In addition to the simulations, our study includes dose-dependent MoS_2 measuremts as well, which will be used to demonstrate the reliability of the theoretical findings in practice.

Funding
Funding from the European Research Council under Grant Agreement 101118656 (ERC Synergy project 4D-BioSTEM) is kindly acknowledged.

Graphic:

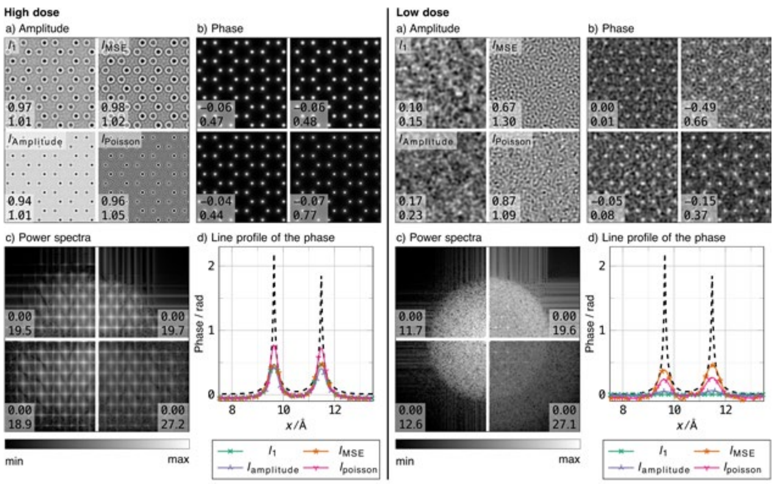

Figure: Left/right reconstruction for the different loss functions as annotated in (a) for the high/low dose case with 10^6/100 electrons per diffraction pattern. (a) - (c) Amplitude, phase and power spectrum for the different loss functions the values indicated in the image are the min and max values. (d) Average line profile of the phase trough a Mo and two S atoms. The phase of the ground truth is shown as a black dashed line in the background.

Keywords:

Loss functions, low-dose, gradient descent

Reference:

[1] Melnyk, Oleh. "Convergence properties of gradient methods for blind ptychography." arXiv preprint arXiv:2306.08750 (2023).
[2] Thibault, Pierre, and Manuel Guizar-Sicairos. "Maximum-likelihood refinement for coherent diffractive imaging." New Journal of Physics 14.6 (2012): 063004.
[3] Lazić, Ivan, et al. "Single-particle cryo-EM structures from iDPC–STEM at near-atomic resolution." Nature Methods 19.9 (2022): 1126-1136.
[4] Zhou, Liqi, et al. "Low-dose phase retrieval of biological specimens using cryo-electron ptychography." Nature communications 11.1 (2020): 2773.

[5] Leidl, Max Leo, Carsten Sachse, and Knut Müller-Caspary. "Dynamical scattering in ice-embedded proteins in conventional and scanning transmission electron microscopy." IUCrJ 10.4 (2023).